mathematics

MDPI

Article

A New Robust Multivariate EWMA Dispersion Control Chart for Individual Observations

Jimoh Olawale Ajadi [1], Inez Maria Zwetsloot [2,*] and Kwok-Leung Tsui [3]

[1] Department of Building and Real Estate, The Hong Kong Polytechnic University, Hung Hom, Kowloon, Hong Kong; ajadi_jimoh2001@yahoo.com
[2] Department of Systems Engineering and Engineering Management, City University of Hong Kong, Kowloon, Hong Kong
[3] Grado Department of Industrial and Systems Engineering, Virginia Tech, Blacksburg, VA 24061-0002, USA; kltsui@vt.edu
* Correspondence: i.m.zwetsloot@cityu.edu.hk

Abstract: A multivariate control chart is proposed to detect changes in the process dispersion of multiple correlated quality characteristics. We focus on individual observations, where we monitor the data vector-by-vector rather than in (rational) subgroups. The proposed control chart is developed by applying the logarithm to the diagonal elements of the estimated covariance matrix. Then, this vector is incorporated in an exponentially weighted moving average (EWMA) statistic. This design makes the chart robust to non-normality in the underlying data. We compare the performance of the proposed control chart with popular alternatives. The simulation studies show that the proposed control chart outperforms the existing procedures when there is an overall decrease in the covariance matrix. In addition, the proposed chart is the most robust to changes in the data distribution, where we focus on small deviations which are difficult to detect. Finally, the compared control charts are applied to two case studies.

Keywords: individual observations; covariance matrix; non-normality; multivariate dispersion chart; EWMA

Citation: Ajadi, J.O.; Zwetsloot, I.M.; Tsui, K.-L. A New Robust Multivariate EWMA Dispersion Control Chart for Individual Observations. *Mathematics* **2021**, *9*, 1038. https://doi.org/10.3390/math9091038

Academic Editor: Timothy M. Young

Received: 26 March 2021
Accepted: 28 April 2021
Published: 3 May 2021

1. Introduction

The quality of a process can often be characterized by multiple correlated variables. For example, when monitoring a patient's systolic and diastolic blood pressure, it is more appropriate to apply one multivariate control chart than two univariate charts. Hotelling [1] introduced the first multivariate control chart. Many researchers have improved on this chart. For example, Lowry et al. [2] proposed a multivariate exponentially weighted moving average (MEWMA), also Crosier [3] developed a multivariate cumulative sum (MCUSUM) chart. Some other researchers introduced multivariate control charts that monitor the variability of a process. For example, Alt [4] proposed a generalized variance chart (GVC). A GVC uses the determinant of the estimated covariance matrix of grouped observations as the monitoring statistics. For details on multivariate dispersion charts for grouped observations, see the review articles by Yeh et al. [5] and Bersimis et al. [6].

Recently, Ajadi and Zwetsloot [7] compared the performance of a multivariate EWMA chart proposed by Huwang et al. [8] for monitoring process variability of individual observations with various charts based on grouped observations. The authors concluded that monitoring methods based on individual observations are quickest in detecting sustained shifts in the process variability. Reynolds Jr and Stoumbos [9] and Reynolds Jr and Stoumbos [10] also advised monitoring with individual observations in the univariate setup.

Ajadi et al. [11] gave an overview of the existing multivariate parametric and nonparametric control charts for monitoring process dispersion of individual observations. Next we briefly introduce some noteworthy examples. Yeh et al. [12] proposed a MaxMEWMV chart.

This chart is developed by computing the difference between the estimated covariance matrix derived from the EWMA statistic and the identity matrix. Then, the L_2-norms of both the diagonal elements and the upper triangular off-diagonal elements are computed. Finally, a single statistic is derived from the two distance-measures to detect changes in the process variability. Huwang et al. [8] proposed the multivariate exponentially weighted mean squared deviation (MEWMS) and the multivariate exponentially weighted moving variance (MEWMV) charts; these charts are based on the trace of the estimated covariance matrix obtained from the EWMA statistic. According to the authors, the MEWMS chart is designed to monitor only changes in the process variability while the MEWMV chart is designed to simultaneously monitors shifts in both the process mean vector and the covariance matrix. Hawkins and Maboudou-Tchao [13] proposed the multivariate exponentially weighted moving covariance matrix (MEWMC) chart. The authors applied the Alt's likelihood ratio statistic to compare the estimated EWMA covariance matrix with the identity matrix. The multivariate control charts discussed above are parametric charts. Li et al. [14] employed a multivariate spatial sign test and EWMA statistic to develop a nonparametric control chart for monitoring shape parameters of the underlying data. The authors named the chart as the multivariate nonparametric shape EWMA (MNSE).

Except for the nonparametric control charts, the other multivariate charts for monitoring the process variability of individual observations are based on the assumption that process data are normally distributed. Stoumbos and Sullivan [15] investigated the robustness of the MEWMA control chart for monitoring process mean vector. The authors showed that the MEWMA control chart is very robust to non-normality even for a highly skewed and heavy-tailed multivariate distributions. Testik et al. [16] extended the work of Borror et al. [17] to examine the robustness properties of multivariate EWMA control charts to non-normal data. Zwetsloot and Ajadi [18] showed that the performance of the univariate EWMA control chart based on logarithm of sample variance is the most robust to normality assumption among three compared univariate EWMA dispersion charts. The authors recommended the chart to be used in practice since it can be difficult to distinguish between normally distributed data, and data that slightly deviates from normality. We have not seen any research that investigate the robustness of the multivariate dispersion charts for individual observations.

Ajadi et al. [11] identified some research directions. One of these is that the robustness of multivariate dispersion charts for individual observations should be investigated. This is one of the motivations for the current study. The objective of this article is to introduce a monitoring method for detecting changes in the process dispersion using individual observations. This method should be robust to slight deviation from the normality assumption. The chart is designed using the logarithm of diagonal elements of the sample covariance matrix estimated using the EWMA statistic. This makes the chart robust to non-normality. In Section 2, we briefly discuss the MaxMEWMV, the MEWMS and a nonparametric control chart. In Section 3, the proposed control chart is discussed in detail. Next, in Section 4, we compare the performance of the proposed chart with the other existing control charts discussed in Section 2. An example is used in Section 5 to support the comparison. Finally, we provide conclusions and recommendations in Section 6.

2. Multivariate EWMA Dispersion Control Charts for Individual Observations

Assume that the data follow a multivariate normal distribution, i.e., $\boldsymbol{X_i} \sim \boldsymbol{N_p(\mu, \Sigma)}$, where the process mean vector and covariance matrix of a p correlated quality characteristics are denoted by $\boldsymbol{\mu}$ and $\boldsymbol{\Sigma}$, respectively. Next, $\boldsymbol{X_i}$ is standardized by transforming it to $\boldsymbol{Y_i}$ as

$$\boldsymbol{Y_i} = \boldsymbol{\Sigma_0}^{-\frac{1}{2}}(\boldsymbol{X_i} - \boldsymbol{\mu_0}) \text{ for } i = 1,\ 2,\ 3,\ \cdots. \tag{1}$$

Thus, $\boldsymbol{Y_i}$ follows a multivariate normal distribution $\boldsymbol{N(\mu_Y, \Sigma_Y)}$, where $\boldsymbol{\mu_Y} = \boldsymbol{\Sigma_0}^{-\frac{1}{2}}(\boldsymbol{\mu} - \boldsymbol{\mu_0})$ and $\boldsymbol{\Sigma_Y} = \boldsymbol{\Sigma_0}^{-\frac{1}{2}}\boldsymbol{\Sigma}\boldsymbol{\Sigma_0}^{-\frac{1}{2}}$. Note that $\boldsymbol{\mu_0}$ and $\boldsymbol{\Sigma_0}$, are the in-control values of $\boldsymbol{\mu}$ and $\boldsymbol{\Sigma}$,

respectively. When the process is in-control, $\boldsymbol{Y_i} \sim \boldsymbol{N_p(0, I_p)}$, where $\boldsymbol{I_p}$ is a $p \times p$ identity matrix. To compute $\boldsymbol{Y_i}$, we need estimates of $\boldsymbol{\Sigma_0}$ and $\boldsymbol{\mu_0}$. These are usually obtained in a Phase I analysis (see Section 3.2 for details).

Next, we discuss two popular parametric (MaxMEWMV, MEWMS) and one non-parametric (MNSE) control charts for monitoring the covariance matrix of individual observations.

2.1. MaxMEWMV Chart

The first multivariate EWMA control chart for monitoring the process variability of individual observations was proposed by Yeh et al. [12]. This chart is referred to as the MaxMEWMV. As Yeh et al. [12] suggested we first transform the data as

$$\boldsymbol{S_i^E} = \lambda \boldsymbol{Y_i Y_i'} + (1 - \lambda)\boldsymbol{S_{i-1}^E}, \tag{2}$$

where $0 < \lambda < 1$ is a smoothing constant and $\boldsymbol{S_0^E} = \boldsymbol{Y_1 Y_1'}$. The monitoring statistic for the MaxMEWMV chart is defined as

$$MaxD_i = max\left(\frac{D_{1i} - E(D_{1i})}{\sqrt{Var(D_{1i})}}, \frac{D_{2i} - E(D_{2i})}{\sqrt{Var(D_{2i})}}\right)$$

where $\boldsymbol{D_i} = \boldsymbol{S_i^E} - \boldsymbol{I_p}$. Note that D_{1i} is the $L_2 - norm$ of the diagonal elements of $\boldsymbol{D_i}$ and D_{2i} is the $L_2 - norm$ of the upper triangular off-diagonal elements of $\boldsymbol{D_i}$. Where D_{1i} is used to detect shifts in the process variance and D_{2i} to detect changes in the correlation structure. The expectation and variance of D_{1i} and D_{2i} are derived analytically by Yeh et al. [12]. A signal is given when $MaxD_i$ exceeds an upper control limit (UCL).

2.2. MEWMS Chart

Later in 2007, Huwang et al. [8] proposed two multivariate EWMA dispersion charts. One of the charts (MEWMS) is designed to detect only changes in the process variability. The MEWMS control chart applies the trace of the estimated covariance matrix obtained from the EWMA statistic ($\boldsymbol{S_i^E}$) as the monitoring statistic.

$$tr(\boldsymbol{S_i^E}) = \Sigma_{k=1}^{p} s_{i,kk}^2$$

where $s_{i,kk}^2$ is the $k - th$ diagonal element of $\boldsymbol{S_i^E}$. The monitoring statistic, $tr(\boldsymbol{S_i^E})$, is compared with the upper and lower control limits (UCL and LCL);

$$LCL/UCL = p \pm L\sqrt{2pc_i}$$

where $c_i = \frac{\lambda}{2-\lambda} + \frac{2-2\lambda}{2-\lambda}(1 - \lambda)^{2(i-1)}$ and L is the control charting constant. The chart signals when $tr(\boldsymbol{S_i^E}) > UCL$ or $tr(\boldsymbol{S_i^E}) < LCL$.

2.3. MNSE Chart

Li et al. [14] incorporated a multivariate spatial sign test with an exponentially weighted moving average (EWMA) scheme to develop a distribution-free control chart for monitoring shape parameters. The authors named the chart the multivariate nonparametric shape EWMA (MNSE) chart. They showed that the MNSE chart is robust to non-normal distributions of the data, in the sense that the in-control performance is not affected. The mean vector ($\boldsymbol{\theta_0}$) and covariance matrix ($\boldsymbol{A_0}$) estimators of the MNSE chart can be obtained simultaneously through Equations (3) and (4).

$$\frac{1}{m}\sum_{j=1}^{m} U\Big(\boldsymbol{A_0}(\boldsymbol{X_j} - \boldsymbol{\theta_0})\Big) = 0 \tag{3}$$

$$\frac{1}{m}\sum_{j=1}^{m} U\Big(\boldsymbol{A_0}(\boldsymbol{X_j}-\boldsymbol{\theta_0})\Big)\, U'\,\Big(\boldsymbol{A_0}(\boldsymbol{X_j}-\boldsymbol{\theta_0})\Big) = \frac{\boldsymbol{I_p}}{p} \tag{4}$$

where m is the size of the historical dataset. The algorithm to compute $\widehat{\boldsymbol{\theta}}_{\boldsymbol{0}}$ and $\widehat{\boldsymbol{A}}_{\boldsymbol{0}}$ estimates from Equations (3) and (4) is available in the supplementary file by Zou and Tsung [19]. Next, Phase II observations, i.e., $\boldsymbol{X_i}, i = 1, 2, 3, \cdots$, can be standardized and transformed by multivariate spatial sign, i.e., $\boldsymbol{Z_i} = U\Big(\boldsymbol{A_0}(\boldsymbol{X_i}-\boldsymbol{\theta_0})\Big)$, where $U(\boldsymbol{x}) = \frac{\boldsymbol{x}}{||\boldsymbol{x}||_2}$ is the spatial sign vector. Then, the EWMA statistic can be computed as

$$\boldsymbol{S_i} = \lambda \boldsymbol{Z_i}\boldsymbol{Z_i'} + (1-\lambda)\boldsymbol{S_{i-1}},$$

where $\boldsymbol{S_0} = \boldsymbol{I_p}/p$. Finally, the monitoring statistic, Q_i in Equation (5), is compared with an upper control limit (UCL).

$$Q_i = \sqrt{\frac{2-\lambda}{\lambda} tr\Big(p\boldsymbol{S_i} - \boldsymbol{I_p}\Big)^2} \tag{5}$$

3. The Proposed Robust EWMA Control Chart

In this section, we introduce our new multivariate dispersion chart for individual observations. The proposed chart is based on the logarithm of the diagonal elements of $\boldsymbol{Y_i}$ and referred to as REWMV, where R is short for robust. We focus on robustness to deviations from the normality assumption that are difficult to identify. As we believe that this is a common situation in practice, data may look approximately normally distributed however it is impossible to verify if they could have slightly heavy tails or if the distribution is a little skewed.

3.1. Guidelines to Implementation of the REWMV Chart

The REWMV control chart incorporates the logarithm of the estimated covariance matrix in the multivariate EWMA statistic. There are three reasons why the logarithm makes the chart more robust. Firstly, as mentioned by Box et al. [20] (Chapter 5.4), the logarithmic transformation of the sample variance is approximately more normally distributed than the sample variance itself. As the logarithm transforms skewed data to approximately normally distributed data. Secondly, Crowder and Hamilton [21] showed that the logarithmic transformation changes the model from a variance shift to a location shift model. This is beneficial as most charts are designed to detect mean shifts quickly. Finally, the variance of the logarithm of sample variance is independent of σ^2 and only depends on sample size.

This idea has been used in univariate monitoring tools quite extensively; Crowder and Hamilton [21] suggested the use of an EWMA scheme to the logarithm transformation of the sample variance for monitoring an increase in the process variability. Shu and Jiang [22] also mentioned that using the logarithm transformation makes the control limits for a two-sided EWMA control chart nearly symmetrical. Zwetsloot and Ajadi [18] compared the performance of three univariate EWMA dispersion charts based on estimated parameters under normal and non-normally distributed data. The authors showed that the EWMA control chart based on logarithm of the sample variance is more robust to non-normality than the other compared charts.

First, we integrate the logarithm of diagonal elements of the estimated covariance matrix into the multivariate EWMA statistic as

$$\boldsymbol{S_i^{logE}} = \lambda\, log\big\{diag\big(\boldsymbol{Y_i}\boldsymbol{Y_i'}\big)\big\} + (1-\lambda)\boldsymbol{S_{i-1}^{logE}}, \tag{6}$$

where $0 < \lambda < 1$, is the smoothing parameter, $\boldsymbol{S_0^{logE}} = E\Big[\boldsymbol{S_i^{logE}}\Big]$ and $diag(A)$ is a vector of the diagonal elements of the matrix A.

Our objective for this study is to detect both increases and decreases in the process variability for multivariate individual observations. Next, we discuss the procedure for the upper and lower-sided monitoring with the proposed REWMV control chart.

The monitoring statistic is reset to a reflection boundary whenever the statistic is less than the boundary for the upper-sided monitoring; or greater than the boundary for the lower-sided monitoring. The reflection boundary $E\left[S_i^{logE}\right]$ is the expected value of S_i^{logE}, and it is obtained as

$$E\left[S_i^{logE}\right] = \begin{bmatrix} -1.27 & -1.27 & \cdots & -1.27 \end{bmatrix}_{p\times 1},$$

under the assumption that $\boldsymbol{Y_i} \sim \boldsymbol{N(0, I_p)}$.

We apply the statistics in Equations (7) and (8) to detect respectively increases and decreases in the process variability. The *max* and *min* in these equations are respectively the element-wise maximum and minimum values of the two vectors.

$$S_i^{log+} = \sum_{k=1}^{p} max\left\{S_i^{logE},\ -1.27\right\}. \tag{7}$$

$$S_i^{log-} = \sum_{k=1}^{p} min\left\{S_i^{logE},\ -1.27\right\}. \tag{8}$$

There are many ways to develop summary statistics to monitor the change of the covariance parameters for multivariate observations. We tried various methods such as taking EWMA statistic before applying logarithm to the estimated covariance matrix; we also employed the mahalanobis distance (a standardized distance measure incorporating the variance of the data) of the estimated EWMA statistic as the summary statistic, among other methods. However, the present method works the best in detecting the considered ranges and types of shifts.

Finally, S_i^{log+} and S_i^{log-} are compared against the upper and lower control limits (*UCL* and *LCL*) to detect upward and downward shifts in the process dispersion respectively.

3.2. Phase I Estimation

To implement our and the other charts, we need estimates of $\widehat{\boldsymbol{\mu}}_{\mathbf{0}}$ and $\widehat{\boldsymbol{\Sigma}}_{\mathbf{0}}$ which we obtain in a Phase I analysis. Many covariance matrix estimators have been employed in the literature for estimating parameters in Phase I. The sample covariance matrix of the pooled observations is the most commonly used covariance matrix, and it is defined as

$$\widehat{\boldsymbol{\Sigma}}_{\mathbf{0}} = \frac{\sum_{j=1}^{m}\left(\boldsymbol{X_j} - \widehat{\boldsymbol{\mu}}_{\mathbf{0}}\right)\left(\boldsymbol{X_j} - \widehat{\boldsymbol{\mu}}_{\mathbf{0}}\right)'}{(m-1)}, \tag{9}$$

where $\widehat{\boldsymbol{\mu}}_{\mathbf{0}} = \frac{\sum_{j=1}^{m} \boldsymbol{X_j}}{m}$ and the observations, $\boldsymbol{X_j}$, are observed at times $j = 1, 2, 3, \cdots, m$. Note that m is Phase I sample size. For each observation of the MEWMS, the MaxMEWMV and the REWMV charts in Phase II, we standardize the data based on the Phase I estimates as

$$\boldsymbol{Y_i} = \widehat{\boldsymbol{\Sigma}}_{\mathbf{0}}^{-\frac{\mathbf{1}}{\mathbf{2}}}\left(\boldsymbol{X_i} - \widehat{\boldsymbol{\mu}}_{\mathbf{0}}\right). \tag{10}$$

Note that, the Phase I estimators for the MNSE chart are obtained through Equations (3) and (4).

4. Performance Comparison

In this section, we compare the performance of the proposed REWMV control chart with the existing competing charts (MaxMEWMV, MEWMS, and MNSE charts). We investigate the robustness of the selected charts to data that is slightly non-normal. We believe this is an important aspect of robustness. Because, as we will show in Section 4.3 it

can be very difficult to distinguish normally distributed data from slightly non-normally distributed data. Hence a monitoring method should perform consistently, however the existing monitoring methods will show many additional false alarms if this slight deviation occurs, as we will show in Section 4.5. But first we discuss the selected performance measures (Section 4.1) and the set-up of our simulation experiments (Section 4.2). Code for obtaining the simulation results is available on github.com/ajadi1982.

4.1. Performance Measures and Control Limits

The performance of the charts is defined in terms of the average of the conditional ARL values ($AARL$). The conditional ARL is defined as the average run length (RL) conditional on a specific Phase I estimate, i.e., $ARL\left[\widehat{\boldsymbol{\Sigma}}_{\mathbf{0}}, \widehat{\boldsymbol{\mu}}_{\mathbf{0}}\right] = E[RL|\widehat{\boldsymbol{\Sigma}}_{\mathbf{0}}, \widehat{\boldsymbol{\mu}}_{\mathbf{0}}]$. We evaluate the conditional ARL for each of the charts with 100 Monte Carlo simulation of the run lengths based on the Phase I parameters. Then, we calculate the mean of 10,000 conditional ARL simulations to obtain the $AARL$. We adjust the control limits for different Phase I sample sizes such that the $AARL_0 = 200$ for $p = 2$, $p = 5$ and $p = 25$. The adjusted control limits for each of the charts at specific values of p, λ and m are provided in Table 1. They are obtained under the assumption that the data are normally distributed.

Table 1. Control limits and control limit constants for the REWMV, MEWMS, the MaxMEWMV, and the MNSE control charts at $AARL_0 = 200$ under normally distributed data.

			REWMV		**MEWMS**	**MaxMEWMV**	**MNSE**
λ	p	m	**LCL**	**UCL**	**L**	**UCL**	**UCL**
0.1	2	50	−4.108	−1.220	2.550	5.200	3.034
		200	−4.230	−1.175	2.475	4.830	2.900
		2000	−4.255	−1.166	2.475	4.600	2.830
	5	50	−8.840	−3.542	3.170	7.900	7.210
		200	−9.173	−3.787	2.638	5.055	6.594
		2000	−9.260	−3.874	2.470	4.210	6.332
	25	50	−34.720	−8.820	20.200	84.270	35.500
		200	−38.970	−21.100	4.930	8.000	28.340
		2000	−40.500	−23.400	2.550	3.700	26.920
0.3	2	50	−6.450	0.060	3.338	7.170	2.700
		200	−6.540	0.076	3.380	6.907	2.660
		2000	−6.570	0.080	3.380	6.740	2.637
	5	50	−12.380	−1.235	3.908	9.240	6.675
		200	−12.700	−1.570	3.260	6.620	6.427
		2000	−12.800	−1.684	3.076	5.900	6.360
	25	50	−42.200	−0.700	17.120	59.00	31.120
		200	−48.000	−13.890	4.670	8.000	27.750
		2000	−49.680	−16.400	2.910	4.700	27.160

4.2. Description of Experiments

Our in-control model is $\boldsymbol{\mu}_{\mathbf{0}} = (0\,0\cdots 0)_{1\times p}$ and $\boldsymbol{\Sigma}_{\mathbf{0}} = \boldsymbol{I}_{\boldsymbol{p}}$. For the out-of-control model, we set a general form $\boldsymbol{\Sigma}_{\mathbf{1}}$ and $\boldsymbol{\Sigma}_{\mathbf{2}}$ for overall and sparse shifts, respectively, as

$$\boldsymbol{\Sigma}_{\mathbf{1}} = \delta \begin{pmatrix} 1 & \rho & \rho^2 & \cdots & \rho^{p-2} & \rho^{p-1} \\ \rho & 1 & \rho & \ldots & \rho^{p-3} & \rho^{p-2} \\ \rho^2 & \rho & 1 & \ldots & \rho^{p-4} & \rho^{p-3} \\ \vdots & \vdots & \ddots & \vdots & \vdots & \vdots \\ \rho^{p-2} & \rho^{p-3} & \rho^{p-4} & \cdots & 1 & \rho \\ \rho^{p-1} & \rho^{p-2} & \rho^{p-3} & \cdots & \rho & 1 \end{pmatrix}, \tag{11}$$

and

$$\boldsymbol{\Sigma_2} = \begin{pmatrix} \delta & \rho & \rho^2 & \cdots & \rho^{p-2} & \rho^{p-1} \\ \rho & 1 & \rho & \cdots & \rho^{p-3} & \rho^{p-2} \\ \rho^2 & \rho & 1 & \cdots & \rho^{p-4} & \rho^{p-3} \\ \vdots & \vdots & \ddots & \vdots & \vdots & \vdots \\ \rho^{p-2} & \rho^{p-3} & \rho^{p-4} & \cdots & 1 & \rho \\ \rho^{p-1} & \rho^{p-2} & \rho^{p-3} & \cdots & \rho & 1 \end{pmatrix}. \tag{12}$$

We consider the following four scenarios for overall or sparse shifts in the process:

- Case 1: overall increase shifts in the variance-covariance matrix
  We increase all the diagonal elements of the covariance matrix (i.e., $\delta > 1$) and/or the correlation coefficients as given in Equation (11).
- Case 2: Sparse increase shifts in the variance-covariance matrix
  We consider increasing shifts in only the first element of the diagonal matrix where $\rho = 0$ and $\rho = 0.3$ as given in Equation (12).
- Case 3: overall decrease shifts in the variance-covariance matrix
  We decrease all the diagonal elements of the covariance matrix (i.e., $\delta < 1$) where $\rho = 0$ and $\rho = 0.3$ as given in Equation (11).
- Case 4: Sparse decrease shifts in the variance-covariance matrix
  We consider decreasing shifts in only the first element of the diagonal matrix where $\rho = 0$ and $\rho = 0.3$ as given in Equation (12).

In addition, we investigate the robustness of the proposed chart and its counterparts. We consider the multivariate *t*- distribution to model high kurtosis (kurtosis measures the thickness of the tails of a distribution), $\boldsymbol{X_i} \sim \boldsymbol{t_p(\nu, \Sigma)}$, where ν is the number of degrees of freedom. We use $\nu = 30$ degrees of freedom. The in-control process mean vector and covariance matrix of $\boldsymbol{X_i}$ are $\boldsymbol{\mu_0}$ and $\frac{\nu}{(\nu-2)}\boldsymbol{\Sigma_0}$ respectively. Since the focus of this study is to monitor the changes in the process variability, the process mean vector remains constant in the out-of-control model while the covariance matrix changes to $\frac{\nu}{(\nu-2)}\boldsymbol{\Sigma_1}$ or $\frac{\nu}{(\nu-2)}\boldsymbol{\Sigma_2}$.

In addition, we employ the multivariate gamma distribution to model high skewness, $\boldsymbol{X_i} \sim \Gamma_p(\alpha, \beta, \boldsymbol{\Sigma})$, where α and β are the shape and scale parameters of the distribution respectively. Throughout this article, we use $\beta = 1$. Note that, for gamma distributed data, the in-control covariance matrix, $\alpha\boldsymbol{\Sigma_0}$, changes to $\alpha\boldsymbol{\Sigma_1}$ (since $\beta = 1$) in the out-of-control model. We employed $\alpha = 16$. Details of the multivariate t and gamma distributions can be found in the appendix of Stoumbos and Sullivan [15].

4.3. How Non-Normal Are the Data?

In this section, we test for the normality of Phase I data simulated for different models using the Henze and Zirkler multivariate normality test. We run 10000 simulations of the test for different values of m; and compute the percentage of the tests that do not reject normality. Table 2 shows the results. We require Phase I sample of $m \geq 500$, $m \geq 1000$ and $m \geq 5000$ for t distributed data with 10, 15 and 30 degrees of freedom respectively to have confidence that the data is non-normal. Moreover, we need $m > 30$, $m > 100$ and $m > 500$ for $\Gamma(1,1)$, $\Gamma(4,1)$ and $\Gamma(16,1)$ respectively to be certain that the skewed data fail the multivariate normality test.

Hence, we see that for small and moderate size Phase I samples it is very challenging and sometimes impossible to distinguish between normal and slight non-normally distributed data. Hence there is a need for control charts that are robust to deviations from the normality assumption. We recommend the use of robust charts when the number Phase I data is less than 500, since testing cannot distinguish between data which is normally or non-normally distributed with high accuracy.

Table 2. Percentage of Henze and Zirkler tests for multivariate normality test that do not reject at a significance level of 0.05.

m	Normal	t_{10}	t_{15}	t_{30}	$\Gamma(1,1)$	$\Gamma(4,1)$	$\Gamma(16,1)$
30	95	86	91	94	2	67	91
50	95	77	87	93	0	39	86
70	95	68	84	92	0	20	81
100	95	58	83	91	0	6	73
150	95	35	72	90	0	0	61
200	95	26	64	89	0	0	48
500	95	0	26	79	0	0	7
1000	95	0	2	62	0	0	0
2000	95	0	0	32	0	0	0
5000	95	0	0	2	0	0	0
6000	95	0	0	0	0	0	0

4.4. Analysis of Phase I Estimators on Different Distributions

In this section, we analyze how the Phase I sample size affects the covariance matrix estimators under different distributions (normal, gamma, t) when the process is in-control. The variability of the trace of the covariance matrix estimates for different values of m is presented in Table 3. We observe that the variability decreases as m increases. The multivariate normal distribution has the least variability when estimating $\hat{\mathbf{\Sigma}}_0$. The non-parametric covariance matrix estimator ($\hat{\boldsymbol{A}}_0$) has similar variability irrespective of the distribution.

Table 3. Variability of the trace for the covariance matrix estimates when $p = 5$.

	$Var(tr(\hat{\mathbf{\Sigma}}_0))$			$Var(tr(\hat{A}_0))$		
m	**Normal**	**Gamma**	**t**	**Normal**	**Gamma**	**t**
10	1.113	1.294	1.371	19.762	22.925	18.020
25	0.417	0.486	0.522	0.206	0.211	0.207
50	0.202	0.243	0.259	0.031	0.032	0.032
75	0.136	0.159	0.171	0.012	0.013	0.012
100	0.101	0.120	0.127	0.007	0.007	0.007
125	0.080	0.095	0.102	0.004	0.004	0.004
150	0.067	0.080	0.086	0.003	0.003	0.003
200	0.050	0.060	0.064	0.001	0.002	0.002

4.5. Performance of the Dispersion Charts

We simulated the $AARL$ values for each of the four competing control charts under the different scenarios discussed in Section 4.2. Results are displayed in Tables 4–7 where gray highlighted values correspond to in-control performance and bold face indicates the best performing chart, i.e., the lowest $AARL_1$ value. The $AARL$ values in italics show the most robust charts to non-normality under in-control performance. For Tables 6 and 7, which show results for the scenarios with decreasing shifts, we set the maximum run length to 10,000 in the simulations for the MEWMS and MaxMEWMV charts. Because these charts are not designed to detect decrease shifts and therefore have extremely long run lengths. This maximum ensures reasonable simulation time. We use an asterisk to indicate any $AARL$-value which is influenced by this maximization and is therefor a underestimate of the actual $AARL$. In addition, we represent $AARL$ values greater than 1000 by > 1000.

4.5.1. Case 1: Overall Increase Shifts in the Variance-Covariance Matrix

For case 1, the results for different number of correlated quality characteristics ($p = 2$, 5, 25) under multivariate normal, gamma and t distributions when $m = 200$ are reported

in Table 4. For small and moderate increases in the process variance, we notice that the MEWMS chart has the best performance among the competing charts. For example, when $p = 25$ and $\delta = 1.1$, the MEWMS chart has the lowest $AARL_1$ value of 42, while the $AARL_1$ of the MaxMEWMV, the MNSE and the REWMV control charts are respectively 63, 203 and 55. In addition, the parametric charts (REWMV, MEWMS, and the MaxMEWMV charts) have almost similar performance at high increase shift ($\delta = 2$) in the process especially for a high value of p.

Table 4. $AARL$ values for an overall increase shift in the process dispersion when $\lambda = 0.3$, and $m = 200$ under multivariate normal, t and gamma distributions. Grey highlighted rows indicate in-control data.

			$p = 2$				$p = 5$				$p = 25$			
Distribution	ρ	δ	**MEWMS**	**MaxMEWMV**	**MNSE**	**REWMV**	**MEWMS**	**MaxMEWMV**	**MNSE**	**REWMV**	**MEWMS**	**MaxMEWMV**	**MNSE**	**REWMV**
normal	0	1.0	203	201	201	200	198	200	197	200	204	196	202	198
		1.1	**108**	119	201	119	**82**	102	197	98	**42**	63	203	55
		1.2	**66**	77	202	78	**43**	59	197	56	**16**	27	203	25
		1.3	**44**	53	202	55	**26**	38	197	37	**9**	14	203	14
		1.5	**25**	30	201	33	**13**	19	198	20	**4**	**6**	202	8
		2.0	**10**	13	203	15	**5**	7	198	9	**2**	**3**	205	**4**
	0.3	1.0	159	**118**	130	165	134	113	**95**	152	132	127	**79**	152
		1.1	91	**78**	131	101	**65**	**65**	94	81	**35**	48	79	48
		1.2	59	**55**	131	68	**37**	42	94	49	**15**	23	79	23
		1.3	**41**	**41**	131	50	**24**	29	94	33	**9**	13	79	14
		1.5	**23**	26	131	31	**13**	17	94	19	**5**	**6**	79	8
		2.0	**10**	12	131	15	**5**	7	94	9	**2**	**3**	78	**4**
gamma	0	1.0	119	120	*203*	*216*	110	87	*198*	220	115	52	*201*	233
		1.1	**75**	80	202	126	**56**	**54**	197	106	32	**26**	202	63
		1.2	**51**	56	204	83	**33**	36	197	61	**14**	**15**	201	27
		1.3	**37**	42	201	58	**22**	26	197	39	**8**	**10**	202	15
		1.5	**23**	26	201	35	**12**	15	197	21	**4**	**5**	201	8
		2.0	**11**	13	203	16	**5**	**7**	198	9	**2**	**2**	200	**4**
	0.3	1.0	106	**88**	131	174	84	**66**	97	163	79	**44**	80	175
		1.1	68	**62**	132	108	47	**43**	94	86	27	**23**	80	54
		1.2	48	**45**	131	73	**30**	**30**	94	52	**13**	**14**	80	25
		1.3	**36**	**35**	130	53	**21**	**23**	94	35	**8**	**9**	81	15
		1.5	**22**	**24**	132	32	**12**	**14**	95	20	**4**	**5**	79	8
		2.0	**11**	**12**	130	15	**6**	**7**	94	9	**2**	**2**	79	**4**
t	0	1.0	134	134	*201*	*203*	101	99	*198*	182	45	43	*202*	98
		1.1	**81**	87	201	123	**54**	60	197	94	**21**	24	203	40
		1.2	**54**	60	204	81	**33**	40	198	56	**12**	15	203	21
		1.3	**39**	45	204	58	**22**	28	200	38	**8**	**10**	202	14
		1.5	**23**	27	201	35	**12**	17	197	21	**5**	**6**	202	8
		2.0	**11**	**13**	199	16	**5**	**7**	199	9	**2**	**3**	204	**4**
	0.3	1.0	116	92	132	168	82	71	96	143	41	37	79	85
		1.1	73	**63**	130	105	**47**	**46**	95	79	**20**	**21**	78	37
		1.2	50	**47**	131	72	**30**	33	95	50	**12**	**14**	79	21
		1.3	**37**	**37**	132	52	**21**	24	95	34	**8**	**10**	78	13
		1.5	**23**	**24**	132	32	**12**	15	94	20	**5**	**6**	79	8
		2.0	**11**	**12**	132	16	**6**	**7**	93	9	**2**	**3**	79	**4**

When the process variances are unchanged (i.e., $\delta = 1$) but the correlation increases ($\rho = 0.3$), the MaxMEWMV chart shows the best performance for $p = 2$ while the MNSE control chart outperforms the other compared charts for $p = 5$ and $p = 25$. When $p = 2$ the MaxMEWMV control chart perform best for simultaneous shifts in both process variances and the correlation. However, the MEWMS control chart has the best performance among the compared charts for $p = 5$ and $p = 25$.

We also observed that $AARL$ values of the REWMV and the MNSE control charts under normal, gamma and t distributions are almost equal for each of the process shifts we consider, i.e. they are robust to deviations from the normality assumption. However, the disadvantage of the MNSE chart is that it does not respond to the overall increase shifts in the process variance; see that all values are approximately 200. The MEWMS and MaxMEWMV control charts are seriously affected by slight deviation from the normality assumption. For instance, $AARL_0$ values of the MEWMS and the MaxMEWMV control charts are respectively 119 and 120 with gamma distributed data. The MEWMS and the MaxMEWMV charts still have the least $AARL_1$ values under the non-normal distributions but note that their in-control performance have the highest rate of false alarms with t and gamma distributions.

4.5.2. Case 2: Sparse Increase Shifts in the Variance-Covariance Matrix

Next, we consider a scenario where only one variable increases. Without loss of generality, we select the first diagonal element of the covariance matrix to changes where $\rho = 0$ and $\rho = 0.3$. Here, we simulated for $\delta = 1.1, 1.2, 1.3, 1.5$ and 2 under multivariate normal, gamma and t distributions, results are reported in Table 5.

Table 5. $AARL$ values for an overall increase shift in the process dispersion when $\lambda = 0.3$, and $m = 200$ under multivariate normal, t and gamma distributions. Grey highlighted rows indicate in-control data.

			$p = 2$				$p = 5$				$p = 25$			
Distribution	ρ	δ	**MEWMS**	**MaxMEWMV**	**MNSE**	**REWMV**	**MEWMS**	**MaxMEWMV**	**MNSE**	**REWMV**	**MEWMS**	**MaxMEWMV**	**MNSE**	**REWMV**
		1.0	203	201	201	200	198	200	197	200	204	196	202	198
		1.1	**145**	152	200	153	162	170	196	172	**187**	**185**	203	**187**
	0	1.2	**107**	115	193	121	**134**	142	191	150	**173**	**172**	200	176
		1.3	**81**	89	186	99	**111**	119	184	131	**159**	**159**	199	165
		1.5	**52**	56	165	71	**77**	81	166	105	138	**127**	191	151
normal		2.0	**23**	**25**	120	39	**38**	**36**	116	68	92	**69**	164	123
		1.0	159	**118**	130	165	134	113	**95**	152	132	127	**79**	152
		1.1	119	**98**	136	129	114	100	**96**	132	124	122	**79**	145
	0.3	1.2	94	**81**	135	105	98	**89**	96	119	115	116	**79**	138
		1.3	74	**67**	134	88	84	**77**	95	106	108	108	**79**	131
		1.5	**48**	**48**	126	66	63	**59**	92	87	97	91	**78**	119
		2.0	**23**	**24**	102	38	35	**31**	74	59	71	**56**	72	100

Table 5. *Cont.*

Distribution	ρ	δ	$p = 2$				$p = 5$				$p = 25$			
			MEWMS	**MaxMEWMV**	**MNSE**	**REWMV**	**MEWMS**	**MaxMEWMV**	**MNSE**	**REWMV**	**MEWMS**	**MaxMEWMV**	**MNSE**	**REWMV**
gamma	0	1.0	119	120	*203*	*216*	110	87	*198*	220	115	52	*201*	233
		1.1	**93**	96	200	164	93	**78**	195	189	107	**49**	201	219
		1.2	**74**	78	195	129	80	**69**	191	164	100	**48**	200	207
		1.3	**60**	63	184	105	70	**61**	185	143	95	**46**	198	195
		1.5	**42**	45	166	75	53	**48**	166	112	82	**40**	193	177
		2.0	**22**	**24**	120	41	31	**28**	115	73	58	**29**	161	142
	0.3	1.0	106	**88**	131	174	84	**66**	97	163	79	**44**	80	175
		1.1	86	**75**	137	138	74	**60**	95	144	76	**43**	79	166
		1.2	69	**63**	135	112	66	**55**	97	127	72	**41**	81	157
		1.3	**56**	**54**	134	93	58	**49**	96	114	68	**39**	80	148
		1.5	**40**	**40**	127	68	46	**40**	92	93	60	**36**	79	136
		2.0	**22**	**23**	101	40	29	**25**	75	64	46	**27**	73	113
t	0	1.0	134	134	*201*	*203*	101	99	*198*	182	45	43	*202*	98
		1.1	**102**	106	198	155	**88**	**88**	197	157	**43**	**41**	203	94
		1.2	**81**	85	195	124	**77**	**78**	191	139	**41**	**41**	202	90
		1.3	**64**	69	184	103	66	69	184	122	**40**	**39**	199	87
		1.5	**44**	48	168	74	**52**	**54**	164	100	**38**	**36**	192	81
		2.0	**22**	**24**	121	42	**31**	**30**	114	67	31	**28**	163	70
	0.3	1.0	116	**92**	132	168	82	**71**	96	143	41	**37**	79	85
		1.1	91	**78**	137	134	73	**65**	97	128	39	**36**	79	82
		1.2	75	**66**	136	110	64	**59**	95	114	38	**35**	79	80
		1.3	60	**56**	136	92	58	**54**	95	103	37	**34**	79	77
		1.5	**42**	**42**	130	69	46	**43**	92	86	34	**32**	78	72
		2.0	**22**	**23**	101	40	29	**26**	73	60	29	**25**	72	63

The MEWMS control chart performs best while the MNSE chart shows the worst performance when detecting only shifts in the process variances. For instance, when $p = 5$ at $\delta = 1.2$ under normally distributed data, the $AARL_1$ for the MEWMS, the MaxMEWMV are respectively 134 and 142, while that of the MNSE and the REWMV control charts are 191 and 150 respectively.

In addition, the MaxMEWMV chart has the best performance for $p = 2$ when the process variances are unchanged but the correction increases ($\rho = 0.3$), while the MNSE control chart outperforms the other compared charts for $p = 5$ and $p = 25$. The MaxMEWMV chart perform best when $p = 2$ and $p = 5$ for simultaneous shifts in the process variance and correlation while the MNSE chart outperforms the other charts for $p = 25$.

Overall, the out-of-control performance of the REWMV control chart is the most robust to non-normality for a sparse increase shift in the process variance among the compared parametric charts.

4.5.3. Case 3: Overall Decrease Shifts in the Variance-Covariance Matrix

We simulated for the overall decrease shifts ($\delta = 0.2$, 0.3, 0.4, 0.6, and 0.8) in the covariance matrix when $\rho = 0$ or $\rho = 0.3$ (case 3). The simulation results for this scenario when $m = 200$ for $\lambda = 0.3$ under multivariate normal, gamma and t distributions are presented in Table 6. The MEWMS and MaxMEWMV control charts are inefficient in detecting decrease shifts in the variance as their $AARL_1$ values in most cases are greater

than 1000. We notice that the REWMV chart has the best performance in detecting overall decrease shifts in the process dispersion.

The MNSE control chart does not react to downward shifts in the process. For example, when $p = 2$ at $\delta = 0.2$ and $\rho = 0$, the $AARL_1$ value of the MNSE chart is 201 and that of the MEWMS and the MaxMEWMV charts are greater than 1000 but the proposed REWMV control chart has the least $AARL_1$ value of 12. In addition, with the t and gamma distributed data, we observe that the REWMV chart is robust to non-normality for the out-of-control performance.

Table 6. $AARL$ values for an overall decrease shift in the process dispersion (case 3) when $\lambda = 0.3$ and $m = 200$ under normal, t and gamma distributions. Grey highlighted rows indicate in-control data.

			$p = 2$				$p = 5$				$p = 25$			
Distribution	ρ	δ	**MEWMS**	**MaxMEWMV**	**MNSE**	**REWMV**	**MEWMS**	**MaxMEWMV**	**MNSE**	**REWMV**	**MEWMS**	**MaxMEWMV**	**MNSE**	**REWMV**
normal	0	1.0	203	201	201	200	198	200	197	200	204	196	202	198
		0.8	> 1000	887 ⋆	202	**125**	> 1000	> 1000	197	**92**	> 1000	> 1000	204	**41**
		0.6	> 1000	> 1000	202	**71**	> 1000	> 1000	200	**39**	> 1000	> 1000	201	**11**
		0.4	> 1000	> 1000	204	**34**	> 1000	> 1000	197	**14**	11	> 1000	198	**4**
		0.3	> 1000	> 1000	202	**21**	> 1000	> 1000	196	**9**	5	> 1000	194	**3**
		0.2	> 1000	> 1000	201	**12**	41	> 1000	193	**5**	4	> 1000	184	**2**
	0.3	0.8	799 ⋆	380	131	**122**	> 1000	522 ⋆	93	**88**	> 1000	> 1000	78	**38**
		0.6	> 1000	> 1000	132	**68**	> 1000	> 1000	92	**37**	> 1000	> 1000	77	**10**
		0.4	> 1000	> 1000	135	**33**	> 1000	> 1000	94	**14**	10	> 1000	79	**4**
		0.3	> 1000	> 1000	133	**21**	711 ⋆	> 1000	94	**9**	5	> 1000	78	**3**
		0.2	> 1000	> 1000	131	**12**	37	> 1000	95	**5**	4	> 1000	75	**2**
gamma	0	1.0	119	120	*203*	*216*	110	87	*198*	220	115	52	*201*	233
		0.8	466	384	202	**129**	822 ⋆	335	196	**93**	> 1000	331	199	**40**
		0.6	> 1000	> 1000	204	**70**	> 1000	> 1000	199	**38**	> 1000	> 1000	202	**11**
		0.4	> 1000	> 1000	203	**35**	> 1000	> 1000	194	**15**	10	> 1000	190	**4**
		0.3	> 1000	> 1000	202	**22**	> 1000	> 1000	195	**9**	5	> 1000	180	**3**
		0.2	> 1000	> 1000	198	**13**	44	> 1000	193	**6**	4	> 1000	156	**2**
	0.3	0.8	353	237	132	**123**	445 ⋆	221	94	**89**	> 1000	268	78	**39**
		0.6	> 1000	> 1000	134	**68**	> 1000	> 1000	95	**37**	> 1000	> 1000	77	**11**
		0.4	> 1000	> 1000	133	**34**	> 1000	> 1000	93	**15**	10	> 1000	76	**4**
		0.3	> 1000	> 1000	136	**21**	> 1000	> 1000	95	**9**	5	> 1000	71	**3**
		0.2	> 1000	> 1000	134	**13**	39	> 1000	91	**5**	4	> 1000	62	**2**
t	0	1.0	134	134	*201*	*203*	101	99	*198*	182	45	43	*202*	98
		0.8	523	412	199	**113**	604 ⋆	372	197	**77**	557	221	205	**29**
		0.6	> 1000	> 1000	199	**64**	> 1000	> 1000	196	**34**	462	> 1000	199	**9**
		0.4	> 1000	> 1000	200	**31**	> 1000	> 1000	198	**13**	10	> 1000	198	**4**
		0.3	> 1000	> 1000	204	**20**	604 ⋆	> 1000	200	**8**	5	> 1000	193	**3**
		0.2	> 1000	> 1000	200	**12**	35	> 1000	197	**5**	4	> 1000	184	**2**
	0.3	0.8	413	241	132	**109**	396	223	95	**74**	420	186	79	**29**
		0.6	> 1000	> 1000	130	**63**	> 1000	> 1000	96	**33**	337	> 1000	78	**9**
		0.4	> 1000	> 1000	134	**30**	> 1000	> 1000	93	**13**	9	> 1000	80	**4**
		0.3	> 1000	> 1000	131	**20**	> 1000	> 1000	96	**8**	5	> 1000	78	**3**
		0.2	> 1000	> 1000	134	**12**	32	> 1000	98	**5**	4	> 1000	77	**2**

4.5.4. Case 4: Sparse Decrease Shifts in the Variance-Covariance Matrix

Consider case 4, where only the first variance decreases, results are displayed in Table 7. The proposed REWMV control chart outperforms the other charts irrespective of the values of p when the sparse decrease shifts are introduced under multivariate normal, gamma and t distributions and $\rho = 0$. The MEWMS and the MaxMEWMV charts show the worst performance among the compared charts. For instance, when $p = 5$ at $\delta = 0.3$, the $AARL_1$ values of the MEWMS, the MaxMEWMV are respectively 714 and 319 under normal distribution; while the REWMV control chart has the lowest $AARL_1$ value of 76. The MNSE chart performs best when there is simultaneously shifts in both process variances and correlations.

The MNSE control chart, again, does not detect any change as the $AARL_0$ values are approximately 200 under multivariate t and gamma distributions. The REWMV chart is the most robust to normality assumption among the compared parametric charts for the out-of-control performance. For instance, the AARL values for the REWMV chart under normal, gamma, and t distributions are respectively 56, 57, and 49 for $p = 5$, $\delta = 0.2$ and $\rho = 0$ while that of MaxMEWMV chart are respectively 319, 117, and 155. However, the excessive rate of false alarm of the MEWMS and MaxMEWMV control charts with the non-normality affect the out-of-control performance of the charts such that their $AARL_1$ are lower than that of the MNSE and the REWMV control charts when $p = 25$.

Table 7. $AARL$ values for a sparse shift in the process variance when $\lambda = 0.3$ and $m = 200$ under normal, t and gamma distributions. Grey highlighted rows indicate in-control data.

Distribution	ρ	δ	$p = 2$				$p = 5$				$p = 25$			
			MEWMS	**MaxMEWMV**	**MNSE**	**REWMV**	**MEWMS**	**MaxMEWMV**	**MNSE**	**REWMV**	**MEWMS**	**MaxMEWMV**	**MNSE**	**REWMV**
normal	0	1.0	203	201	201	200	198	200	197	200	204	196	202	198
		0.8	432	354	187	**155**	298	265	189	**169**	241	208	203	**179**
		0.6	896 *	592 *	150	**114**	426	304	167	**135**	266	213	196	**160**
		0.4	> 1000	784 *	89	**75**	622 *	314	128	**98**	321	227	186	**135**
		0.3	> 1000	817 *	60	**55**	730 *	319	109	**76**	349	227	179	**115**
		0.2	> 1000	807 *	**36**	**37**	847 *	319	88	**56**	360	228	173	**96**
	0.3	0.8	297	172	**115**	149	182	131	**88**	159	150	135	**77**	163
		0.6	542 *	253	**84**	107	251	153	**76**	124	173	141	**75**	149
		0.4	943 *	401	**46**	69	320	173	**58**	89	192	148	**71**	125
		0.3	> 1000	550	**31**	50	356	181	**50**	69	199	150	**70**	108
		0.2	> 1000	711 *	**18**	33	407	185	**40**	50	220	145	**65**	89
gamma	0	1.0	119	120	*203*	*216*	110	87	*198*	220	115	52	*201*	233
		0.8	215	191	190	**156**	146	**104**	188	168	133	**54**	200	175
		0.6	358	277	151	**118**	193	**116**	165	136	145	**55**	191	158
		0.4	522	325	90	**76**	229	118	129	**99**	162	**56**	183	133
		0.3	588 *	329	60	**57**	259	121	110	**77**	174	**56**	177	115
		0.2	660 *	331	**37**	**39**	290	117	88	**57**	179	**54**	174	97
	0.3	0.8	166	125	**113**	151	105	**76**	89	160	86	**45**	78	161
		0.6	280	170	**83**	109	130	87	**76**	127	98	**45**	75	147
		0.4	405	244	**46**	69	153	92	**59**	88	102	**47**	72	123
		0.3	456	269	**31**	51	170	90	**51**	71	104	**47**	69	107
		0.2	529	322	**18**	34	182	93	**40**	51	115	**47**	67	88

Table 7. *Cont.*

Distribution	ρ	δ	$p = 2$				$p = 5$				$p = 25$			
			MEWMS	**MaxMEWMV**	**MNSE**	**REWMV**	**MEWMS**	**MaxMEWMV**	**MNSE**	**REWMV**	**MEWMS**	**MaxMEWMV**	**MNSE**	**REWMV**
t	0	1.0	134	134	*201*	*203*	101	99	*198*	182	45	43	*202*	98
		0.8	232	210	192	**140**	137	**120**	190	142	48	**44**	202	107
		0.6	434	320	149	**105**	177	134	166	**113**	51	**47**	194	98
		0.4	733 *	424	91	**68**	226	149	129	**81**	55	**47**	184	82
		0.3	908 *	463	60	**51**	261	151	108	**67**	58	**48**	179	74
		0.2	> 1000	462	**36**	**35**	287	155	85	**49**	59	**50**	175	63
	0.3	0.8	189	123	**114**	136	106	**83**	86	131	42	**39**	77	101
		0.6	315	173	**80**	99	130	92	**75**	104	46	**40**	76	90
		0.4	500	257	**46**	62	160	102	**60**	76	49	**41**	72	79
		0.3	616 *	312	**30**	47	179	110	**50**	59	52	**42**	69	70
		0.2	751 *	420	**18**	31	200	115	**40**	44	53	**42**	67	60

4.6. Further Investigation on Robustness

In this section, we want to investigate the robustness of the charts to non-normality under the in-control performance, results are displayed in Figure 1. We employed t distribution with different degree of freedom (15 up to 50) to model moderate to high kurtosis for the 4 considered multivariate EWMA dispersion charts. We notice that the proposed chart has the most robust performance among the three parametric charts because its $AARL_0$ is closest to 200. Moreover, its performance is almost similar to the MNSE chart.

In addition, we observe that for all the values of α we considered for the gamma distributed data, the proposed REWMV and the MNSE charts have approximately $AARL_0 = 200$. In general, the MaxMEWMV and the MEWMS charts show the worst performance in terms of their robustness to non-normally distributed data.

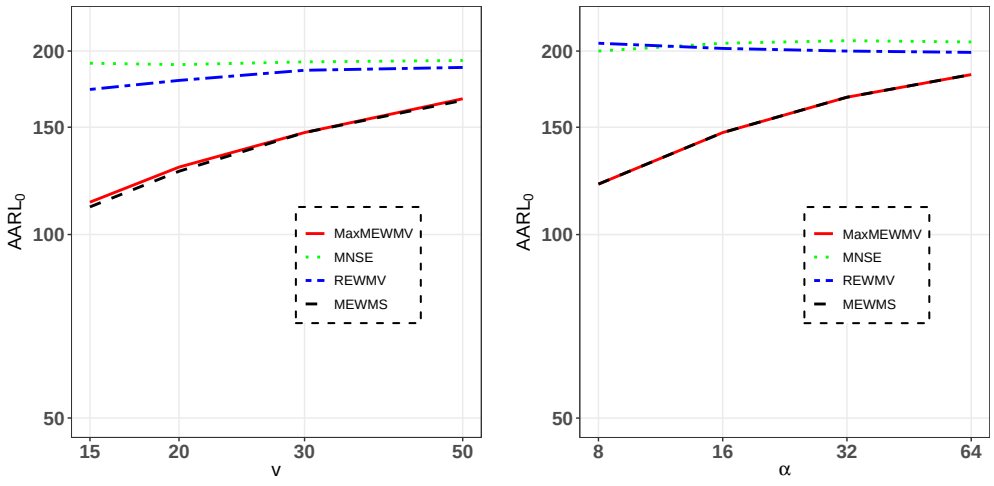

(**a**) t distribution (**b**) gamma distribution

Figure 1. In-control $AARL$ for each of the compared multivariate EWMA dispersion charts for individual observations versus degree of freedom in (**a**) and shape parameter in (**b**). Charts are designed with $\lambda = 0.1$, $m = 50$ for $p = 2$ and an UCL from Table 1 using normally distributed data.

Overall, in Tables 4–7 and Figure 1, we notice that the REWMV and MNSE control charts consistently show the most robust performance to non-normality in the in-control. However, the MNSE shows very poor performance for overall shifts in the process variance.

The MEWMS and MaxMEWMV control charts have the best performance for increase shifts in the process variances, only if the data is perfectly normally distributed. However, the proposed REWMV control chart shows the best performance for the overall decrease shifts in the process variances and comparable performance to the MEWMS and MaxMEWMV charts for increases. In addition it shows robust performance if the data show small deviation from normality.

5. Examples

In this section, we demonstrate how to apply the proposed multivariate dispersion charts to real applications. We consider two different datasets; one healthcare and one industrial application.

5.1. Example to Monitor Elder Care Center Dataset

In this section, we employed the daily measurement of systolic blood pressure (SBP), see Zwetsloot and Ajadi [18] for details about the dataset. Zwetsloot and Ajadi [18] show that the data deviates slightly from the normality assumption. In this section, we arrange the dataset as multivariate individual observations where we select five elders. The first 30 multivariate observations (i.e., $m = 30$ for $p = 5$) are employed to estimate the process parameters. The Phase I estimates are computed based on Equation (9), we obtain the estimated process mean vector and sample covariance matrix ($\widehat{\boldsymbol{\Sigma}}_{\mathbf{0}}$) respectively as

$$\widehat{\boldsymbol{\mu}}_{\mathbf{0}} = \begin{pmatrix} 121.9 & 128.1 & 111.8 & 124.7 & 133.1 \end{pmatrix},$$

$$\widehat{\boldsymbol{\Sigma}}_{\mathbf{0}} = \begin{pmatrix} 113.706 & -34.301 & 9.037 & -19.175 & 55.147 \\ -34.301 & 187.099 & 6.395 & 33.294 & -46.246 \\ 9.037 & 6.395 & 55.013 & -3.444 & 13.361 \\ -19.175 & 33.294 & -3.444 & 94.202 & -16.671 \\ 55.147 & -46.246 & 13.361 & -16.671 & 237.995 \end{pmatrix}.$$

Moreover, for the MNSE chart, the estimated location and scatter matrix are obtained through Equations (3) and (4):

$$\widehat{\boldsymbol{\theta}}_{\mathbf{0}} = \begin{pmatrix} 121.1 & 129.7 & 111.2 & 124.9 & 132.5 \end{pmatrix},$$

$$\widehat{\boldsymbol{A}}_{\boldsymbol{\rho 0}} = \begin{pmatrix} 1 & 0.071 & -0.264 & 0.311 & -0.196 \\ 0 & 0.646 & 0.032 & -0.359 & 0.121 \\ 0 & 0.000 & 1.129 & 0.112 & -0.005 \\ 0 & 0.000 & 0.000 & 0.859 & 0.032 \\ 0 & 0.000 & 0.000 & 0.000 & 0.443 \end{pmatrix}.$$

Due to a change in the measurement system, for details see Zwetsloot and Ajadi [18] and Mahmood et al. [23], there is a downward shift in the process variance from 12 February 2018 onwards. We try to detect this change with the different charts.

We construct a two-sided REWMV chart and the other competing charts for Phase II monitoring where the in-control $AARL$ is fixed at 100 for $\lambda = 0.1$. We obtained the control limits for the MEWMS, the MaxMEWMV and the MNSE charts respectively as 3.17, 8.4, and 7.26. In addition, the control chart's constants for the REWMV chart in the upper- and lower-sided monitoring are respectively -2.964 and -9.13, where the reflection boundary is -6.35, i.e., $\sum_{i=1}^{p} E[logD_i] = -1.27p$ for $p = 5$.

Figure 2 displays the charts. It is obvious from Figure 2a,b that there is no signal received for detecting decrease shifts in the covariance matrix with the MEWMS and MaxMEWMV control charts, which is inline with the simulation results. Figure 2d shows that the REWMV chart first signals (three out-of-control signals) for decrease shifts in the process during the shifted period of the SBP measurement. Moreover, we observe in Figure 2c that the MNSE chart triggers one signal on 2 March 2018. This supports our simulation results in Section 4.5 that the proposed REWMV control chart is very effective in detection of decrease shifts in the covariance matrix when data are normally distributed or possibly slightly skewed or heavy tailed.

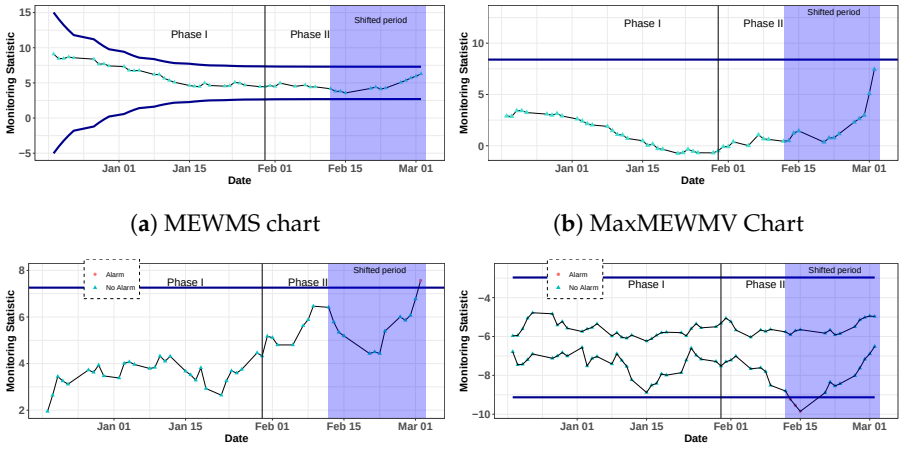

(**a**) MEWMS chart (**b**) MaxMEWMV Chart

(**c**) MNSE Chart (**d**) REWMV Chart

Figure 2. Monitoring SBP multivariate data with the four compared charts.

5.2. Industrial Application

We also employed an industrial dataset collected from a mechanical process to monitor process dispersion of the compared charts. The dataset is available from the MSQC package in R; see Santos-Fernández [24] for details. The Phase I dataset (mech1) contains 45 individual observations ($m = 45$) with seven correlated quality characteristics ($p = 7$). Based on this, we compute the phase I estimates; we also obtained the control limits for the charts respectively as 3.5, 8.75, and 9.56 for the MEWMS, the MaxMEWMV and the MNSE control charts. In addition, the control chart's limits for the REWMV chart in the upper- and lower-sided monitoring are respectively -4.55 and -12.1. These control limits are obtained based on $m = 45$ at $\lambda = 0.1$ that satisfy $ARL_0 = 100$.

Next, we applied the mech2 (Phase II) dataset for online monitoring. Figure 3 shows the charts applied to the Phase II data. We noticed that the MaxMEWMV chart detects no signal in the process variability where the MEWMS chart first detects increase shifts in the covariance matrix at observations 22 and 25. The MNSE chart detects a shift at observation 39 and the REWMV control chart signals for a decrease shift at 46. As we do not know if or when the data is out-of-control it is impossible to tell which chart is signalling a false alarm or which chart has signalled a shift quickest.

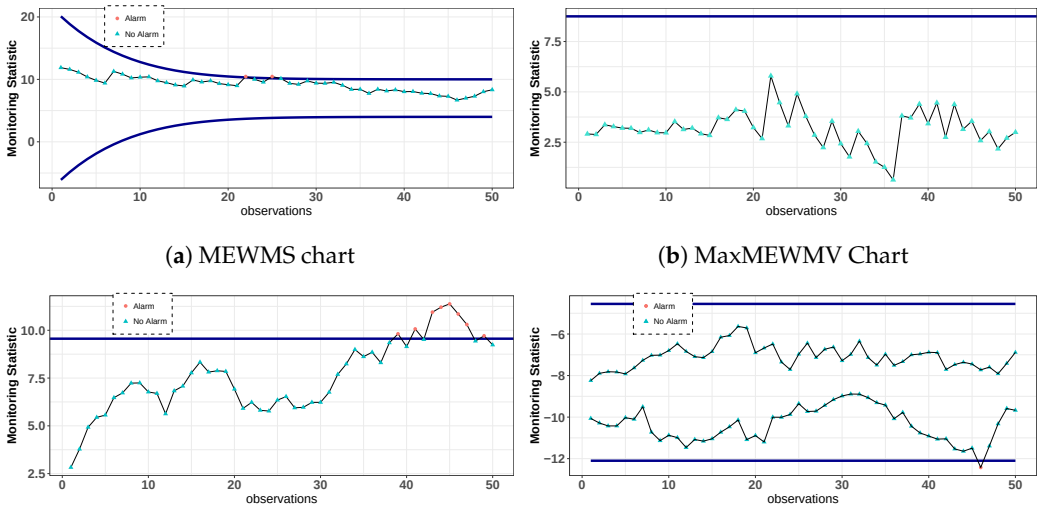

(**a**) MEWMS chart (**b**) MaxMEWMV Chart

(**c**) MNSE Chart (**d**) REWMV Chart

Figure 3. Monitoring SBP multivariate data with the four compared charts.

6. Conclusions and Recommendation

In this paper, we introduced the REWMV control chart, a chart that is effective in detecting changes in the process dispersion when monitoring multivariate processes based on individual observations. The chart is robust to slight deviations from the normality assumption and guarantees in-control performance as expected and reasonable quick shift detection. It does not suffer from excessive false alarms like most method. This chart applies the logarithm to the covariance matrix. The REWMV is a new robust multivariate dispersion chart. We compared the performance of the REWMV control chart with some existing multivariate EWMA dispersion charts based on estimated parameters under normally and non-normally distributed data.

The REWMV chart outperforms the other competing charts when there is an overall decrease shift in the covariance matrix and shows comparable performance for increase shifts. In general, the MEWMS and the MaxMEWMV control charts have bad performance for a decrease in the process variances, while they show the best performance among the compared charts for an increase shifts in covariance matrix. Moreover, the performance of the non-parametric MNSE chart is bad for an overall increase or decrease in the process dispersion.

Next, we investigated the robustness of the REWMV control chart and the other multivariate EWMA dispersion charts for individual observations. We showed that the in-control performance of the MaxMEWMV and MEWMS control charts suffers from an excessive rate of false alarms with the gamma and t distributions. Both the MNSE and the REWMV control charts are robust to non-normality under in-control and out-of-control performance, where the MNSE chart is almost perfectly distribution free.

We apply only the constant control limits for monitoring the proposed REWMV chart by using two separate charts for detecting upward and downward shifts in the process dispersion. However, we recommend the use of probability limits for future work to enhance simultaneous monitoring of both increase and decrease shifts in the covariance matrix. In addition, in this article, we are only restricted to monitoring the process mean vector and covariance matrix, however, other shape parameters shifts may also be investigated for monitoring the REWMV charts.

The focus of this paper is on monitoring process variability with individual observations, however, the proposed chart can as well be extended to monitoring grouped observations where the sample covariance matrix of the grouped observations are incorporated in the EWMA statistic of Equation (6). Moreover, we can extend this study by investigating the robustness of some Phase I covariance matrix estimators to outliers with the proposed REWMV control chart. In addition, integrating two multivariate control charts to detect the process mean vector and covariance matrix simultaneously sometimes loses the ability to provide detailed diagnostic information when a process is out of control. Hence, the performance of the proposed REWMV chart can be investigated when monitoring such out-of-control scenario.

Author Contributions: Methodology, I.M.Z. and J.O.A.; Formal analysis, I.M.Z.; Supervision, K.-L.T.; Writing–original draft, J.O.A. All authors have read and agreed to the published version of the manuscript.

Funding: We are thankful to the Centre of Systems Informatics Engineering (CSIE) of City University of Hong Kong for their support and for supplying the data used as illustrating healthcare case in this paper. The data are part of a larger project partly supported by Research Grants Council Theme-Based Research Scheme [T32-102-14N] and City University of Hong Kong [9610406]. The work of I.M. Zwetsloot was partially support by the City University of Hong Kong [7005090,705567].

Institutional Review Board Statement: Not applicable.

Informed Consent Statement: Not applicable.

Data Availability Statement: Data sharing not applicable.

Conflicts of Interest: The authors declare no conflict of interest.

Sample Availability: The R code for the simulations in this article is available on the github page of the author with account ajadi1982.

References

1. Hotelling, H. Multivariate Quality Control Illustrated by the Air Testing of Sample Bomb Sights, Techniques of Statistical Analysis, Ch. II. In *Selected Techniques of Statistical Analysis for Scientific and Industrial Research, and Production and Management Engineering*; McGraw-Hill: New York, NY, USA, 1947; pp. 111–184.
2. Lowry, C.; Woodall, W.; Champ, C.; Rigdon, S.E. A multivariate exponentially weighted moving average control chart. *Technometrics* **1992**, *34*, 46–53. [CrossRef]
3. Crosier, R.B. Multivariate generalizations of cumulative sum quality-control schemes. *Technometrics* **1988**, *30*, 291–303. [CrossRef]
4. Alt, F.B. Multivariate quality control. *Encycl. Stat. Sci.* **1985**, *6*, 110–122.
5. Yeh, A.B.; Lin, D.K.; McGrath, R.N. Multivariate control charts for monitoring covariance matrix: A review. *Qual. Technol. Quant. Manag.* **2006**, *3*, 415–436. [CrossRef]
6. Bersimis, S.; Psarakis, S.; Panaretos, J. Multivariate statistical process control charts: An overview. *Qual. Reliab. Eng. Int.* **2007**, *23*, 517–543. [CrossRef]
7. Ajadi, J.O.; Zwetsloot, I.M. Should observations be grouped for effective monitoring of multivariate process variability? *Qual. Reliab. Eng. Int.* **2020**, *36*, 1005–1027. [CrossRef]
8. Huwang, L.; Yeh, A.B.; Wu, C.W. Monitoring multivariate process variability for individual observations. *J. Qual. Technol.* **2007**, *39*, 258–278. [CrossRef]
9. Reynolds, M.R., Jr.; Stoumbos, Z.G. Control charts and the efficient allocation of sampling resources. *Technometrics* **2004**, *46*, 200–214. [CrossRef]
10. Reynolds, M.R., Jr.; Stoumbos, Z.G. Should observations be grouped for effective process monitoring? *J. Qual. Technol.* **2004**, *36*, 343–366. [CrossRef]
11. Ajadi, J.O.; Wang, Z.; Zwetsloot, I.M. A review of dispersion control charts for multivariate individual observations. *Qual. Eng.* **2021**, *33*, 60–75. [CrossRef]
12. Yeh, A.; Huwang, L.; Chien-Wei, W.U. A multivariate EWMA control chart for monitoring process variability with individual observations. *IIE Trans.* **2005**, *37*, 1023–1035. [CrossRef]
13. Hawkins, D.M.; Maboudou-Tchao, E.M. Multivariate exponentially weighted moving covariance matrix. *Technometrics* **2008**, *50*, 155–166. [CrossRef]
14. Li, Z.; Zou, C.; Wang, Z.; Huwang, L. A multivariate sign chart for monitoring process shape parameters. *J. Qual. Technol.* **2013**, *45*, 149–165. [CrossRef]
15. Stoumbos, Z.G.; Sullivan, J.H. Robustness to non-normality of the multivariate EWMA control chart. *J. Qual. Technol.* **2002**, *34*, 260–276. [CrossRef]
16. Testik, M.C.; Runger, G.C.; Borror, C.M. Robustness properties of multivariate EWMA control charts. *Qual. Reliab. Eng. Int.* **2003**, *19*, 31–38. [CrossRef]
17. Borror, C.M.; Montgomery, D.C.; Runger, G.C. Robustness of the EWMA Control Chart to Non-Normality. *J. Qual. Technol.* **1999**, *31*, 309–316. [CrossRef]
18. Zwetsloot, I.M.; Ajadi, J.O. A comparison of EWMA control charts for dispersion based on estimated parameters. *Comput. Ind. Eng.* **2019**, *127*, 436–450. [CrossRef]
19. Zou, C.; Tsung, F. A multivariate sign EWMA control chart. *Technometrics* **2011**, *53*, 84–97. [CrossRef]
20. Box, G.E.P.; Hunter, W.; Hunter, J. *Statistics for Experimenters*, 1st ed.; John Wiley and Sons: New York, NY, USA, 1978.
21. Crowder, S.V.; Hamilton, M.D. An EWMA for Monitoring a Process Standard Deviation. *J. Qual. Technol.* **1992**, *24*, 12–21. [CrossRef]
22. Shu, L.; Jiang, W. A New EWMA Chart for Monitoring Process Dispersion. *J. Qual. Technol.* **2008**, *40*, 319–331. [CrossRef]
23. Mahmood, T.; Wittenberg, P.; Zwetsloot, I.M.; Wang, H.; Tsui, K.L. Monitoring data quality for telehealth systems in the presence of missing data. *Int. J. Med Inform.* **2019**, *126*, 156–163. [CrossRef]
24. Santos-Fernández, E. *Multivariate Statistical Quality Control Using R*; Springer Science & Business Media, Germany Science & Business Media: Berlin/Heidelberg, Germany, 2012; Volume 14.